Rheology of confined granular flows : from gas to glass

J-F. Métayer*, R. Delannay*, P. Richard*, A. Valance* and M. Y. Louge†

*IPR, Université de Rennes 1, CNRS UMR 6251, F35042 Rennes Cedex, France
†Sibley School of Mechanical and Aerospace Engineering, Cornell University, Ithaca, NY 14853 USA

Abstract. An intriguing feature of granular matter is the close coexistence of solid-like regions and liquid-like flows. We study steady, fully-developped, granular flows confined between parallel vertical sidewalls. The sidewall friction stabilizes the underlaying heap at an inclination exceeding the angle of repose and increasing with flow rate. Our experiments reveal, in agreement with numerical simulations, that the volume fraction varies strongly in the flowing layer. We show that the resultant sidewall friction is not constant either. Above a critical depth, solid volume fraction, velocity and friction evolve on a common length scale. Below, the system appears to behave as a glass engaged in creeping flow.

Keywords: <Enter Keywords here>
PACS: 45.70.-n, 64.70.P-

INTRODUCTION

Although kinetic theory captures the behavior of dilute granular flows, the theoretical attempts made to describe dense granular flows, and in particular the necessity to take into account enduring contacts [1, 2] are still matter of debate. Pouring continuously grains at the top of a granular heap allows one to observe all the states of granular matter: from gaseous state (close the the free surface) to a quasistatic state (deep inside the flow). It is thus the ideal experiment to test existing theories or to inspire new ones. Lemieux and Durian illustrated this by pouring grain between parallel, flat, frictional sidewalls, thus creating a flow of relatively small angle of inclination near jamming [3]. At steeper angles, Taberlet et al. [4] observed a thin, rectilinear, steady, fully-developped, agitated layer riding atop a static heap forming spontaneously at an inclination exceeding the angle of repose and increasing with flow rate (Fig. 1). For these “Sidewall Stabilized Heaps” (SSH), they showed how sidewall friction allows the flowing layer to sustain the heap at an anomalous angle; without such friction, the flow is less steep and governed by the nature of the base [5]. Although common in channel avalanches and silos, confined shear flows have elicited less attention than those without sidewalls. Here, we report a large scale experimental study on grain displacements in a confined granular pile exhibiting a steady surface flow. By combining two experimental methods (particle tracking and γ-densitometry) we are able to obtain the streamwise velocity and solid volume fraction profiles [5]. A previous study, using mainly molecular dynamics simulation([6]), revealed that, downward along y, the flow feature distinct regions: (1) a nearly collisionless zone where grains describe ballistic trajectories; (2) a flowing layer with mostly invariant shear rate and a solid volume fraction gradually increasing on a scale l_v; (3) a dense quasistatic pile where velocity, volume fraction and wall friction vary on the same characteristic length l_v; (4) beneath a critical depth $\propto l_v$, a creeping, glassy zone. In this paper we show that numerical simulations of the flow and experiments are in good agreement. We also give additionnal information concerning the intermittent motion of grains in the glassy zone.

EXPERIMENTS

Our experimental set-up (Fig. 1) consists of two 1200×1200 mm parallel and vertical glass plates separated by width W. Glass-beads of diameter $d = 500 \pm 100\,\mu$m are continuously poured between these plates through a "double-hopper". The lower hopper is continuously filled with particles by the upper one. The aperture of the lower hopper precisely controls the input flow rate Q, defined as the mass of material entering the channel per unit of time and per unit of width. In such a set-up, Q and W are the only control parameters. We set $W = 9d$. When the system reaches a steady-sate, the input flow rate is equal to the output flow rate which is measured using an electronic scale weighting the material falling out of the channel. All our experiments are conducted in a temperature and humidity-controlled room (20° C and 50% of humidity). In order to minimize electrostatic effects the material is passed through a metal sieve connected to the ground prior to all experiments. The beads are painted in black to limit light reflection. A Photron APX RS camera of 1024×1024 resolution for 50 to 30,000 Hz frame rate tracks rapid grains, a Nikon D200 reflex camera at 12 images/minute was used for slow grains. This range of frequency is large enough to track grains whose velocity is between 3.10^{-4} m/s and 10 m/s (fast camera)

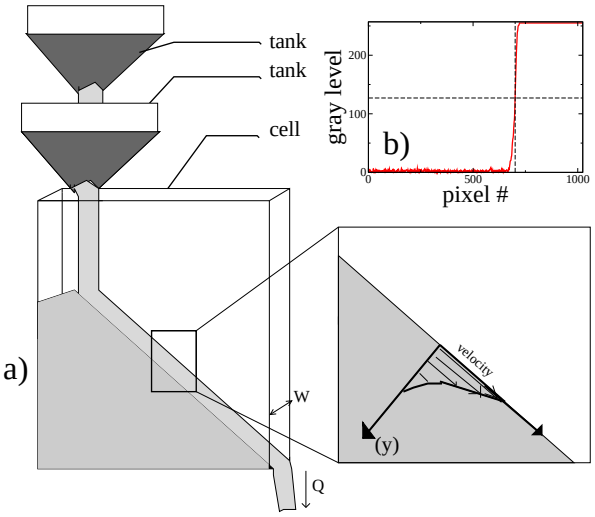

FIGURE 1. (a) Sketch of the experimental set-up. The cell is totally closed on its bottom and on the left side, so that the beads can form pile on which a flow takes place. The (x,y,z) axes are defined as follows: x is the direction of the flow, y is perpendicular to the free surface and directed downwards and z is perpendicular to the sidewalls. (b) Gray level profile along y direction of a picture obtained with the fast camera. The free surface position is defined as the middle of the sharp variation i.e. when the grey level is equal to 127.

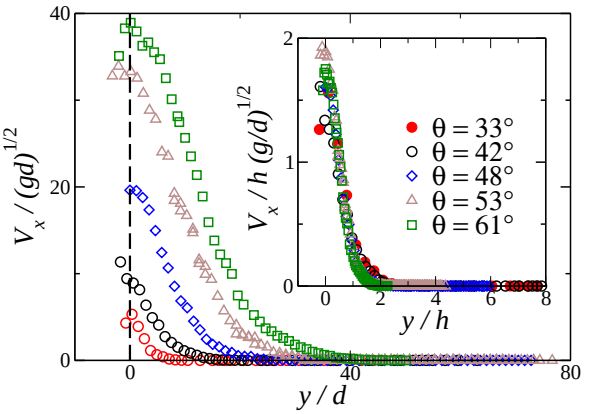

FIGURE 2. Stream-wise velocity V_x profiles for different angles of inclination of the free surface; Inset: same curves where the horizontal axis is made dimensionless using the height of the flowing layer h and the vertical one using the characteristic velocity $V_x/(h\sqrt{g/d})$.

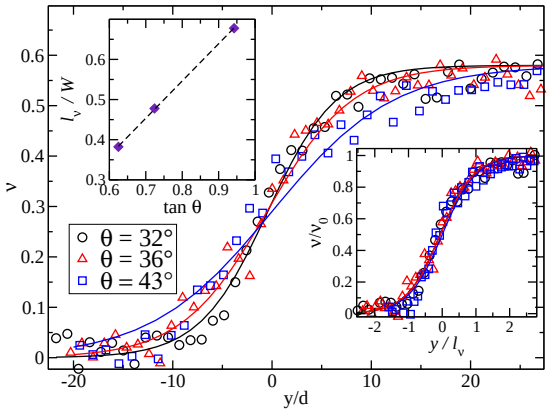

FIGURE 3. Profiles of volume fraction ν at inclinations shown vs. depth; the right inset shows how ν/ν_0 vs. y/l_ν collapses on a master curve; left inset: variations of the scale l_ν with $\tan\theta$.

and between 3.10^{-2} m/s and 1.10^{-6} m/s (camera). The bead size is about 30 pixels, a tracking program deduces the velocity of a given grain from the difference between its successive positions, assuming that the tracked grains motion is less that one radius between two images. To estimate the precision of our measures, and the smaller velocity we can detect, the position of grains in an immobile packing have been tracked. The displacements measured are artifacts due to spot light variations inducing fluctuations in the gray level of each pixel. The minimum average velocity that can be detected is then $f/200$ mm.s^{-1} where f is the frequency of the camera. The position of the free surface is deduced from the gray level profile along y, by image processing. Since this profile varies sharply for zero (black) to 256 (white) at the free surface, its position is defined as the middle of this variation, i.e. when the gray level is equal to 127 (Fig. 1b). The angle of inclination of the free surface, θ is also measured by image processing.

The packing fraction is deduced from the absorption of γ-rays by the granular material. The channel is placed between the source of γ-rays (Cs137) and a scintillator which measures the intensity of the beam. This intensity follows the Beer-Lambert law: $I(y) = I_0 \exp(-\alpha W \nu(y))$, where I_0 is the intensity measured when the channel is empty, α the absorption constant which depend on the material ($\alpha = 0.188$ cm^{-1} for glass), W the channel width and ν the packing fraction averaged in the direction z perpendicular to the sidewalls.

RESULTS

The streamwise velocity profile for grains close to the lateral glass walls in these areas are reported Fig. 2 for different angles of the free surface (and thus different flow rates). In the flowing region, these profiles are almost linear (except close to the free surface for large angles of inclination). The shear rate is therefore constant and independent of the inclination angle. This can be proved by plotting $V_x/h\sqrt{g/d}$ as a function of y/h (inset of Fig. 2), where h is the height of the flowing layer

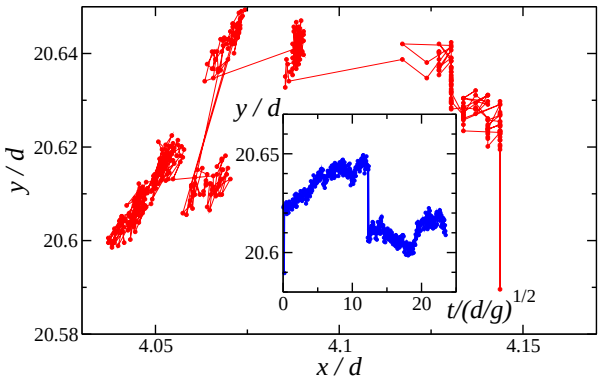

FIGURE 4. Trajectory of a grain initially located at $y \approx 3l_v$. Inset: variation of its depth with dimensionless time.

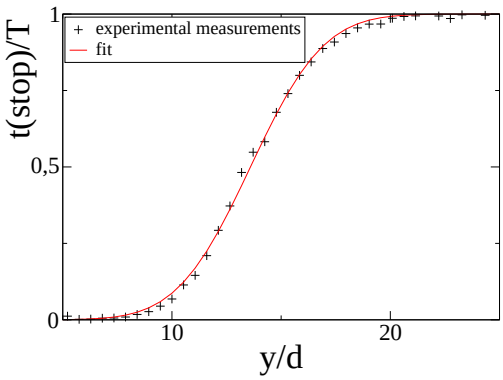

FIGURE 5. Variation of the rest time of grains with the depth. $W = 19d$, $Q = 5400$ grains/(d.s), the time-step is equal to $1/3000s$. The continuous line corresponds to a fit by the function (4) with $b = 13.5d$ and $c = 3.7d$.

measured as the distance between the free surface and the intersection between the tangent of the linear part of the profile and the y axis. At this stage, it is important to note that the same scaling is also valid for numerical simulations of these experiments [6]. Figure 3 shows profiles for the volume fraction ν along the downward direction y perpendicular to the free surface. Two distinct regions can be clearly identified: a quasi-static region with a volume fraction approaching 0.58, toped by a flowing layer where the volume fraction decreases drastically as one approaches the free surface. The packing fraction profiles can be very well fitted by an exponential function of the following form:

$$\nu(y) = \frac{\nu_0}{2}\left[1+\tanh(y/l_v)\right] = \frac{\nu_0}{1+\exp(-2y/l_v)} \qquad (1)$$

ν_0 and l_v are fitting parameters and correspond respectively to the packing fraction in the quasi-static region and to the characteristic length scale over which the packing fraction varies. Note that the origin of the y axis has been chosen such that $\nu(y=0) = \nu_0/2$, ν_0 and l_v completely characterize the packing fraction profiles. If the y coordinate is made dimensionless using the length scale l_v instead of the grain diameter d, all the curves collapse on a master curve which is nothing but a tangent hyperbolic function. We find that the packing fraction in the quasi-static region is independent of the inclination angle and equal to $\nu_0 = 0.58$, while the length scale l_v increases linearly with the tangent of the inclination angle (cf. left inset of Fig. 3):

$$\frac{l_v}{W} = 1.2 \times [\tan\theta - \tan\theta_0] \qquad (2)$$

with $\theta_0 \approx 20°$. We obtained the same fits from the numerical simulation results, with similar values of the fitting parameters [6]. In both cases, we note that the region of constant shear rate extends over approximatively twice the characteristic length scale l_v and one can therefore use the latter to define the height h of the flowing region (more precisely, $h \approx 1.7l_v$). Equation (2) is thus equivalent to the simple relation between the flow inclination and the relative height h/W of the flowing layer:

$$\tan\theta = \tan\theta_0 + \mu_w(h/W)\,, \qquad (3)$$

where θ_0 and $\mu_w \approx 1/(1,7\nu)$ are interpreted respectively as an internal friction angle of the granular material and an effective friction coefficient at the side walls that accounts for rolling or sliding contacts [4]. At very high inclination angles, a very dilute layer of constant velocity appears on the top of the flow. In this top layer, the particles have ballistic trajectories experiencing rare collisions. Deeper in the flow (i.e., $l_v < y < 3l_v$), the streamwise velocity exhibits an exponential decay with a characteristic length scale l_v. Further down in the quasi-static region, the decay remains exponential but it is drastically reduced [6]. In this part also, the tracking method we used allows to follow grains that are close to lateral walls. Fig. 4 reports the trajectories of grains. The plot represents the successive positions of the particles tracked in each image. For grains that are in the creeping region (Fig. 4) we clearly observe fluctuating motion that reveals a caging motion: The grains seems to be trapped in a finite area before escaping and being trapped again. The evolution of y with time (4, inset) confirms the presence of quick rearrangements between two long periods of trapping. Similarly to what is observed during granular compaction [7] a large motion is not a motion from one cage to another one, but a cage deformation. The quick rearrangements observed become less and less frequent as one goes deeper in the flow.

A remarkable point is that for all the frame rates we used, the mean displacement corresponding to the "large"' motion of a grain is the same, it shows that

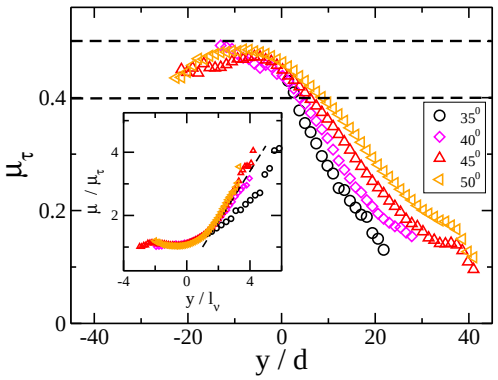

FIGURE 6. Variation of μ_τ with depth in the simulations of [6] for several θ. The top horizontal line marks the microscopic friction μ, and the lower the apparent wall friction $\mu_w = 1/(2\eta)$. The inset reveals a master curve of μ/μ_τ vs. y/l_v, which becomes linear for $y/l_v > 2$ (dashed line).

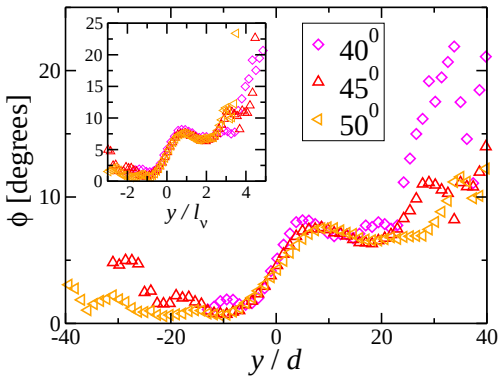

FIGURE 7. Variation of the orientation of the sidewall friction $\vec{\tau}_w$ across the depth for different inclination angles in the simulations. Inset: ϕ versus the dimensionless depth y/l_v.

grains move during a time shorter than our smallest time-step ($1/15000$ s in those experiments). Moreover this "'elementary"'displacement of a grain is independent of its depth and is very small ($\approx 1/50\,d$) compared to the particle diameter. For each grain we have measured the ratio between the number of time-steps for which no displacement is detected: t(stop) and the total number T of recorded time-steps ($T = 200$ for each grain). Fig. 5 shows this ratio averaged over grains at the same depth. At the top of the flow the grains move continuously (t(stop) $= 0$), deeper in the pile the ratio increases to approach 1, it reveals the gradual transition from a liquid to a solid behavior. The ratio profile can be well fitted by an error function (see fig. 5).

$$f(x) = 0.5\,\mathrm{erf}(\frac{y-b}{c}) + 0.5, \qquad (4)$$

where b and c are fitting parameters. The coefficient b characterizes the depth of the transition and the coefficient c its length.

<DISCUSSION>

The "'cage"' motion of the grains allows to predict the decrease of the sidewall friction with depth. While trapped, grains describe a random oscillatory motion, thus contributing negligibly to the mean resultant wall friction force $\vec{\tau}_w$. As trapping duration grows with depth, the resultant wall friction weakens. This decrease may seem surprising but it is essential to ensure the momentum balance in the deep part of the system [6]. Numerical simulations [6] confirm clearly that the macroscopic friction coefficient $\mu_\tau \equiv ||\vec{\tau}_w||/|\sigma^w_{zz}|$, defined as the ratio of shear to normal stress at the wall, weakens with depth (see fig. 6). The full characterization of the sidewall friction requires in addition the knowledge of its direction ϕ: $\vec{\tau}_w \equiv -\,||\vec{\tau}_w||(\cos\phi\,\vec{x} + \sin\phi\,\vec{y})$. Fig. 7 shows that friction is pointed against the flow in the flowing layer: $0 < \phi < 5°$; in the static pile, it rotates progressively with depth but $\cos\phi$ remains close enough to 1 that friction hardly contributes to the force balance along y. In other words, the "Janssen effect" is negligible. This is in agreement with the observed trajectories in creeping zone (fig. 4) showing that brief and binary collisions predominate rather than long-lived contacts.

ACKNOWLEDGMENTS

This work was supported by ANR grant (ANR-05-BLAN-0273), NSF travel grant INT-0233212 and CNRS (PICS France-USA). The authors thank G. Le Caër and P. Sanchez for fruitful conversations.

REFERENCES

1. P. C. Johnson and R. Jackson, *J. Fluid Mech.* **1**76, 67 (1987).
2. M. Y. Louge, *Phys. Rev. E.* **6**7, 061303 (2003).
3. P.-A. Lemieux and D. J. Durian, *Phys. Rev. Lett.* **85**, 4273–4276 (2000).
4. N. Taberlet, P. Richard, A. Valance, W. Losert, J-M. Pasini, J. T. Jenkins and R. Delannay, *Phys. Rev. Lett.* **91**, 264301(2003).
5. R. Delannay, M. Y. Louge, P. Richard, N. Taberlet and A. Valance, *Nature Materials* **6**, 99 (2007).
6. P. Richard, A. Valance, J.F Métayer, P. Sanchez, J. Crassous, M. Louge and R. Delannay, *Phys. Rev. Lett.* **101**, 248002 (2008).
7. P. Ribière, P. Richard, R. Delannay, D. Bideau, M. Toiya, and W. Losert, *Phys. Rev. Lett.* , 268001 (2005).